HHS Public Access

Author manuscript

Pain. Author manuscript; available in PMC 2020 September 01.

Published in final edited form as:

Pain. 2019 September ; 160(9): 2161–2171. doi:10.1097/j.pain.0000000000001583.

Modulation of Brain Networks by Sumatriptan-Naproxen in the Inflammatory-Soup Migraine Model

James Bishop[1,2,5], **Lino Becerra**[1,2,3], **Gabi Barmettler**[1,2], **Pei-Ching Chang**[1,2], **Vanessa Kainz**[4,†], **Rami Burstein**[4,†], **David Borsook**[1,2,3]

[1]Pain/Analgesia Imaging Neuroscience (P.A.I.N.) Group, Department of Anesthesia, Boston Children's Hospital, Center for Pain and the Brain, Harvard Medical School, Boston, MA, USA;

[2]Athinoula A. Martinos Center for Biomedical Imaging, Massachusetts General Hospital, Charlestown, MA, USA;

[3]Departments of Psychiatry and Radiology, Massachusetts General Hospital, Harvard Medical School, Charlestown, MA 02129, USA;

[4]Department of Anaesthesia and Critical Care, Beth Israel Deaconess Medical Center, Harvard Medical School, Boston, MA 02215, USA;

[5]Department of Radiology, Stanford University School of Medicine, Stanford, CA 94305.

Keywords

fMRI; rat; migraine; resting state networks; anti-inflammatory; triptans; CNS; translational

Introduction

The development of pre-clinical models of migraine or headache-like behaviors contribute to the understanding of cellular and molecular neurobiology of the disease. Pre-clinical models that parallel mechanistic aspects of migraine promote the development of novel pharmacological compounds for therapeutic interventions and identification of potential clinical biomarkers to characterize therapeutic response. The well-established rodent 'inflammatory soup' (IS) model [9; 30; 39; 40], reproduces hallmark features of clinical migraine populations including structural [20] and functional [3] brain alterations. It is postulated that neuronal sensitization and extracranial hypersensitivity are chemical-mediated features of the migraine condition. While the mechanisms underlying the release of such mediators remain undetermined, animal models that mimic these pathophysiological processes, such as the IS model, provide a valuable platform for pre-clinical investigations. Specifically, application of IS to the dura matter produces robust sensitization of trigeminal primary afferents, consistent with central sensitization, while also leading to cutaneous mechanical and thermal allodynia. IS is comprised of an acidic mixture of pro-inflammatory compounds including serotonin (5HT), bradykinin, histamine, and prostaglandin (PGE2),

Corresponding Author: David Borsook, M.D., Ph.D., Pain/Analgesia Imaging Neuroscience (P.A.I.N.) Group, Department of Anesthesia, Boston Children's Hospital, Boston, MA 02215, USA, Tel: 781 216 1199, David.Borsook@childrens.harvard.edu.
[†]Co-Last Authors

which when applied directly to the dura mater, activates the trigeminovascular system and potentiates neuronal sensitization and neurogenic neuroinflammation [9; 40]. Similar pathological processes occur in clinical migraineurs and have been proposed to influence connectivity of large-scale brain networks.

Neuroimaging studies in clinical migraine populations have demonstrated substantial deviations in cerebral perfusion, alterations in structural and functional brain networks important for pain gating, modulation, and homeostasis, and a general increase in allostatic load [7; 27; 34]. Using the rodent IS model to reproduce clinical features, we have previously reported the feasibility to elicit and measure 'ictal-like' dural sensitization within the MRI environment sufficient to evoke functional network changes. Resting state network (RSN) alterations during IS migraine induction in conscious rats were consistent with many network alterations observed in clinical populations, including the default mode network (DMN), autonomic (AN), executive (EN), basal ganglia (BG), and cerebellar (CN) networks [3]. These findings validate the IS migraine model to replicate neurological migraine symptoms and supports its use for investigating changes in functional networks underlying pharmacological therapies.

Sumatriptan and naproxen sodium are widely used pharmacological migraine therapies that are more effective when administered in combination [15; 22]. Sumatriptan is a 5HT-$1_{B/D}$-receptor agonist belonging to the triptan drug class [33] and naproxen sodium is a COX-1 and COX-2 inhibitor, enabling downstream anti-inflammatory effects by inhibiting prostaglandin synthesis [11]. Together these compounds mitigate migraine symptoms by reducing neurogenic inflammation, diminishing neuronal excitability and eliciting vasoconstriction [22]. Given their known therapeutic efficacy, the pharmacological influence of these drugs on functional brain networks during a migraine attack has been poorly characterized.

In this study we sought to investigate sumatriptan/naproxen induced network level alterations utilizing fMRI in a rat inflammatory soup model (IS) compared to control animals that receive synthetic interstitial fluid (SIF). We hypothesized that sumatriptan/naproxen administration would globally reduce network activity in IS compared to SIF animals by reducing neuronal excitability and inflammation, and inducing vasoconstriction. To the best of our knowledge, this is the first fMRI study in an animal model of migraine to examine functional alterations in response to sumatriptan/naproxen treatment. By capturing the effect of sumatriptan and naproxen on brain networks following migraine induction, these data provide insight into the neural targets of drug efficacy and provide a potential biomarker or 'fingerprint' for novel pharmacological compounds.

Methods

Experimental Design

The study was approved by the Massachusetts General Hospital Institutional Animal Care and Use Committee (IACUC). Twenty-four male Sprague-Dawley rats (Charles River Labs, Wilmington, MA), weighing approximately 300–350 grams, were used for these experiments. Animals were first acclimated to the MRI scanning environment and imaging

procedure for three consecutive days. Following the acclimation period, each animal underwent a surgical procedure to implant an extradural catheter just deep to the skull. Prior to placement into the MRI scanner, twelve animals received migraine induction via an injection (20μL) of inflammatory soup and twelve animals were administered a control vehicle consisting of synthetic interstitial fluid (SIF) [40]. Subsequent conscious fMRI data were collected consisting of resting state, thermal, and mechanical acquisitions before and after pharmacological administration of sumatriptan/naproxen via tail vein infusion.

MRI Acclimation

Rats were behaviorally acclimated to the imaging cradle, head fixation apparatus, and MRI environment during three consecutive training sessions (days 1, 2 and 3). In each session, rats were lightly anesthetized with 2% Isoflurane, positioned into custom MRI body cradles and imaging headgear, and placed in a mock MRI box for one hour. During this time the animals were exposed to potential environmental olfactory stimuli within the scanner room and the full range of MRI sounds performed on the day of data collection.

Dural Cannulation

Dura cannulation was performed as previously described in Becerra et al., 2017. In brief, on day 3 following MRI acclimation, each rat was surgically implanted with an indwelling cannula just superior to the dura mater. Anesthesia consisted of 2% isoflurane induction followed by a single mixed IP injection of ketamine (50 mg/kg), Xylazine (5 mg/Kg), and Acepromazine (1 mg/Kg). All animals also received a single subcutaneous injection of Atropine (0.1 mg/ml) to mitigate respiratory secretions. Each animal was then head-fixed utilizing a stereotaxic device and wrapped in a circulating water heating pad to maintain physiological temperature. A small midline (anterior to posterior) incision was made to expose the skull as well as the lambda to bregma cranial sutures. Using a surgical microscope for guidance, a graded trough was fashioned to the right of the sagittal suture using a micro drill to expose the dura mater just anteriorly to the lambda suture. A PE-10 cannula (PE 10) was then inserted into the trough using caution to place it on top of the dura without damaging the meningeal tissue. The body of the cannula was then secured to the intact skull using dental cement. The remaining loose end was threaded under the skin, and extended out of a small incision at the anterior portion of the face, superior and medial to the whisker pad. The exterior portion of the tubing was heat-sealed to prevent infection and to allow injection of IS or SIF on the day of imaging.

Dural Stimulation

On experimental day five, 90 minutes prior to the start of the MRI acquisition, IS migraine induction or SIF vehicle was administered topically onto the dura mater (Figure 1). The IS solution contained 1 mM histamine, 1 mM serotonin, 1 mM bradykinin, and 0.1 mM prostaglandin E_2 (pH 5.5). The modified SIF contained 135 mM NaCl, 5 mM KCl, 1 mM $MgCl_2$, 5 mM $CaCl_2$, 10 mM glucose and 10 mM Hepes (pH 7.2). First, the heat seal of the cannula was trimmed several millimeters followed by injection 20 μL of either IS or SIF over a 20 second interval (~1 μL/s). After the injection was completed, the tubing was again resealed using glass-bead sterilized forceps to ensure that there was no loss of either SIF or IS.

Conscious MRI Setup

One hour following dura mater stimulation, rats were briefly anesthetized via 2% Isoflurane for 15 minutes. During this time a tail-vein cannula was inserted for subsequent pharmacological infusion of sumatriptan/naproxen within the MRI. Rats were then positioned in a custom made MRI body cradle and ear bars made to fit in the depression between the angle of the mandible and the anterior border of the sternocleidomastoid muscle. Lastly, headgear with a bite bar was positioned over the ear bars and placed in a larger, open tubular apparatus that secured the headgear and prevented head motion.

MRI Acquisition

Anatomical: Immediately following setup, awake animals were placed into the MRI and anatomical images were acquired with a RARE sequence (24 1.0 mm slices, TR/TE = 4000/40.5 ms, 128×128 in-plane resolution with FOV of 30 mm) in a 4.7 T Bruker BioSpec Scanner (Bruker, Billerica, MA). At 90 minutes post-IS/SIF infusion, functional MRI began (Figure 1).

Pharmacological (Sumatriptan & Naproxen Infusion) Infusion Scan: A 15 minute functional infusion scan was obtained was acquired using an EPI sequence with the following parameters: 15 Slices 1.5 mm thick, TR/TE = 3000/12 ms, FOV: 3cm, 64×64, 300 time points. Functional MRI data was continuously collected during Sumatriptan and Naproxen infusion, which was administered separately through a tail vein catheter at 5 and 6 minutes respectively. Both injections were administered over a one minute duration with identical 1mg/kg rat drug concentrations. Given the pH differences between the two substances, Sumatriptan and naproxen were administered separately to avoid potential precipitation out of solution.

MRI Analysis

Functional images were processed with FSL 4.1.9 (FMRIB's Software Library, www.fmrib.ox.ac.uk/fsl) as previously described [5]. The following preprocessing steps were performed: 1) Images were motion corrected (MCFLIRT) and underwent spike detection (fsl_motion_outliers). Motion profiles were inspected to determine potential differences between IS and SIF groups and were deemed acceptable for subsequent analysis if head-motion was less than 0.5mm. The number of motion correction generated spikes for IS (M=24.1, SD=8.3) and SIF (M=25.3, SD =3.9) cohorts; t(0.42)=, p=0.68 were not significantly different between groups and were used as regressors of non-interest. 2) De-skulling to isolate brain from the skull and non-brain soft tissue by first manually drawing a brain mask for each animal and then using the subsequently generated binary mask to perform brain extraction (BET). In our experience, manual brain extraction outperforms automated segmentation. 3) Motion and spike artifacts were removed from the data by regressing out the six motion parameters and the spike explanatory variables identified in step 1 (above). 4) Next, the images were spatially smoothed using a Gaussian Kernel FWHM filter of 0.7 mm and high-pass filtered (HPF) at 0.01 Hz threshold. Registration of fMRI images to standard space was the conducted using the FSL's FLIRT tool. Standard space consisted of an anatomical scan from a single rat with the following imaging

parameters: matrix size of 256×128×24 with a voxel size of 0.117×0.117×1 mm^3. Independent component analysis (ICA) was run at the individual level and inspected for components with temporal profiles that resembled motion correction plots. Individual components were further spatially inspected to identify and remove motion-related activity (e.g. edge effect activity). These components were removed utilizing FSL tools (fsl_regfilt). De-noised data were then concatenated and an ICA-based group decomposition was calculated to determine 40 components using the FSL melodic tool. Group differences between IS and SIF were calculated using a random model approach and statistical significance was determined with a false-discovery-rate enhanced mixture model approach [32].

Network Identification

Networks for healthy rats, previously described in the literature [5], including the cerebellar, default mode network, basal ganglia loops, sensorimotor and autonomic networks, were used as templates for component identification from the total group ICA decomposition. A spatial Pearson correlation coefficient was calculated between each component and the templates to quantify goodness-of-fit. Correlation coefficients larger than 0.25 were considered significant and were used to determine correspondence between components and specific RSN templates. Significant components were visually inspected to confirm similarity with published data. RSN scans were then processed with a dual regression approach to determine changes in co-activation of whole brain with identified networks [16]. Group statistical maps for each component were determined with a randomized approach [16] and statistical significance accounting for multiple comparisons was determined with a combined mixture-model and false discovery rate method [32]. The resulting identified networks are displayed in Figure 2; Tables 1–6.

Results

Network responses to Sumatriptan/Naproxen treatment following induction of migraine-like pathophysiology (IS) or control (SIF) were captured following using functional magnetic resonance imaging and analyzed in twenty-four animals. Each animal received topical administration of either IS (migraine; n=12) or SIF (sham; n=12) to the dura mater followed by intravenous administration of 1mg/kg Sumatriptan/Naproxen via tail vein catheter over a period of two-minutes during fMRI evaluation. There was no indication of differences in motion parameters during image acquisition between the groups.

Pharmacological effects on brain networks: IS vs. SIF

Pharmacological infusion of Sumatriptan/Naproxen produced significant between-group (IS vs. SIF) alterations in functional connectivity across several networks including the cerebellar, default mode, basal ganglia, autonomic, and salience networks (Figure 2). Connectivity differences with respect to functional networks are highlighted in Tables 1–6 and displayed in Figure 2.

Cerebellar Network: Though relatively understudied, migraine dysfunction associated with cerebellar involvement includes motor (ataxia, loss of coordination, and hemiplegia),

visual (nystagmus, saccade alterations, and diplopia), and vestibular (vertigo) manifestations [43]. Consistent with these symptoms, the cerebellum receives afferent input from the trigeminal ganglia and the trigeminal spinal nucleus while also projecting to neural structures that have been widely associated with pain and migraine (thalamus, hypothalamus, PAG, etc.) [23]. Compared to SIF controls, IS animals exhibited diminished cerebellar network connectivity with in the cingulate cortex, the spinal trigeminal nucleus, the forelimb region of the primary somatosensory cortex, the secondary visual cortex, the secondary motor cortex, the olfactory cortices, and cerebellar lobules 2,3, and 6. Conversely, the IS cohort did not demonstrate any significant increases in connectivity compared to the SIF cohort within the cerebellar network.

Default Mode Network (DMN): The DMN consists of a set of constitutively active brain regions that have been identified to have a critical role in the regulation of cognitive and behavioral responses. Alterations in DMN connectivity have been demonstrated during ictal [13] and interictal [41] phases of migraine. Both increases and decreases in connectivity were identified between IS and SIF groups within the default mode network. IS treated animals exhibited decreased connectivity compared to SIF controls in default mode network regions including the cerebellar lobule 6, the subicular complex of the hippocampal formation, the simple lobule, crus 2 of the ansiform lobule, the nucleus of the lateral lemniscus, the primary auditory cortex, perirhinal cortex, the posterior area of the parietal cortex, and the jaw and trunk regions of the primary somatosensory cortices. Following Sumatriptan/Naproxen infusion, IS treated animals displayed increased connectivity compared to SIF controls within the cingulate cortex, spinal trigeminal nuclei, the secondary motor cortex, the laterobasal amygdaloid nuclear complex and the inferior colliculus.

Basal Ganglia Network: The basal ganglia network facilitates the integration of thalamo-cortical structures involved in pain processing and is speculated to be a hub of adaptive neuroplasticity [26]. Compared to SIF controls, IS treated animals demonstrated increased functional connectivity within the basal ganglia network compared to SIF animals in the following regions: the simple lobule, primary motor cortices, the cerebellar lobule 5, perirhinal cortex, the lateral olfactory cortices, secondary auditory cortex, bilateral laterobasal amygdaloid nuclear complex, the temporal association cortex, ventral pallidum, primary visual cortex, cingulate cortex, the secondary somatosensory cortex, the primary somatosensory cortex including the barrel field, the forelimb region of the primary somatosensory cortex, the olfactory amygdala, and the paramedian lobules. Conversely, compared to SIF controls, IS treated animals did not exhibit reduced functional connectivity in any regions within the basal ganglia network.

Autonomic Network: Autonomic dysfunction, including alterations in both sympathetic and parasympathetic pathways have been described in migraineurs and it has been suggested that the condition may lead to heightened sensitivity these networks [28]. Between-group (IS vs. SIF) comparisons in functional connectivity demonstrated both increases and decreases in functional connectivity following Sumatriptan/Naproxen infusion. Compared to SIF controls, IS animals demonstrated increased functional connectivity within the autonomic network between the following structures: paramedian lobules, paraflocculus, superior

colliculus, CA1 field of the hippocampal formation, the barrel field of the primary somatosensory cortex, the lateral olfactory cortex, crus 2 of the ansiform lobule, cerebellar lobule 7, special sensory cranial nuclei, and bilaterally within the vomeronasal amygdala. Alternatively, following sumatriptan/naproxen infusion, IS animals exhibited decreased connectivity compared to SIF controls within the inferior colliculus, lobule 5 of the cerebellum bilaterally, the retrosplenial cortex, the lateral olfactory cortices, the simple lobule, the paraventricular zone of the hypothalamus, the reticular formation of the midbrain, perirhinal cortex, the subicular complex of the hippocampal formation, the secondary visual cortex, the forelimb region of the primary somatosensory cortex, and the posterior area of the parietal cortex.

Sensorimotor Network: The sensorimotor network is important for both perception and sensory qualities of the migraine condition which may be collectively linked to pain discrimination [48]. Between-group connectivity alterations were observed within the sensorimotor networks following sumatriptan/naproxen infusion. Rats pretreated with IS to induce migraine-like pathophysiology revealed increased connectivity in the following regions compared to SIF controls: cerebellar lobules 2, 7 (bilateral), and 9, the spinal trigeminal nuclei, bilaterally within the crus 2 of the ansiform lobule, the hindlimb (bilateral), upper lip (bilateral), and trunk region of the primary somatosensory cortex, the posterior nucleus of the thalamus, the raphe nuclei of the midbrain, the paramedian lobule, the temporal association cortex, the lateral olfactory cortices, the primary motor cortex, cingulate cortex, the copula of the pyramis, the primary visual cortex, secondary visual cortex, the inferior colliculus, secondary somatosensory cortices, the lateral zone of the hypothalamus, the superior colliculus. Decreased connectivity in IS animals compared to SIF controls was observed in the following regions: secondary motor cortex, perirhinal cortices, secondary visual cortex, primary motor cortex, superior and inferior colliculi, the lateral group of the septal region, pretectum, and the trigeminal nerve.

Salience Network: The salience network is a collection of brain structures that are involved in regulating attention to internal and external stimuli and may be disrupted in migraineurs from both the conditions or from medications used to treat it [1]. Within the salience network, functional connectivity was increased in animals pretreated with IS to induce migraine-like pathophysiology compared to SIF control animals in the simple lobules. Alternatively, IS animals displayed reduced functional connectivity compared to the SIF cohort in the following regions: cerebellar lobule 7, the medial zone of the hypothalamus, the olfactory amygdala, secondary somatosensory cortices, lateral olfactory cortices, paraflocculus, the temporal association cortex, superior colliculus, secondary motor cortices, the CA1 field of the hippocampal formation, the jaw region of the primary somatosensory cortex, and the crus 2 of the ansiform lobule. Where is the effect of the sumatriptan/naproxen treatment after infusion of IS?).

Discussion

The current study describes the first pre-clinical fMRI investigation to identify whole-brain network alterations following sumatriptan/naproxen pharmacological intervention in the IS migraine model. Specifically, we demonstrated that administration of IS followed by

sumatriptan/naproxen infusion produced changes within functional brain networks including: default mode, basal ganglia, autonomic, sensorimotor, cerebellar, and salience networks.

IS Migraine Induction, Network Alterations, and Pharmacological Intervention

Epidural application of IS has been shown to produce behavioral hallmarks of migraine such as facial allodynia in freely moving rats, presumably a result of the development of sensitization in peripheral and central trigeminovascular networks [9; 10; 14; 30; 44]. In our previous whole-brain fMRI investigation in conscious rodents, we identified robust cortical and subcortical network alterations following single IS dural exposure during resting state and following punctate mechanical stimulation [3]. Similarly, Jia and colleagues revealed functional connectivity changes between the periaqueductal grey, a key anatomical structure for pain modulation, and nodes of the pain matrix following chronic IS injection [21]. Together this literature supports the robustness of the IS model to produce effects consistent with clinical reports [41; 42; 45; 46], and suggests increased neuronal excitability and tactile hypersensitivity during migraine [7].

Given the complexity of migraine pathophysiology, diverse pharmacological targets have been exploited to relieve headache symptoms, often requiring a combination of medications, such as sumatriptan and naproxen. Sumatriptan is a 5-$HT_{1B/1D}$ antagonist with vasoconstrictive properties, that is postulated to influence nociception by disrupting communications between peripheral and central trigeminovascular neurons in the spinal trigeminal nucleus [24]. Naproxen is a non-selective COX inhibitor that interferes with sensitization and inflammation by blocking cyclooxygenase subsequently preventing prostaglandin synthesis from arachidonic acid [31; 37]. The anti-nociceptive effects of naproxen have been well characterized in the IS migraine model. For example, single unit recordings in the trigeminal ganglion of IS treated animals suggest that sensitization of the peripheral meningeal nociceptors is suppressed following naproxen infusion [25]. Alternatively, abolishment of burst activity and neuronal hyper-responsiveness was observed within the medullary dorsal horn in IS treated animals following naproxen infusion [19]. Together, these studies indicate that naproxen mitigates both the peripheral and central sensitization components of migraine pathophysiology.

Significance of brain network alterations in IS and sham treated animals following sumatriptan/naproxen administration:

The *Default mode Network (DMN)* is a collection of constitutively active, task-independent, neural regions critical for the regulation of dynamic brain states such as attention and emotional processing [35]. We previously demonstrated increased DMN functional connectivity to both cortical and subcortical regions in the rat IS model [3]. This finding corresponds with work conducted by Coppola and colleagues who report increased DMN resting state functional connectivity in migraineurs during spontaneous migraine attack compared to healthy volunteers. Meanwhile, others have identified prolonged DMN connectivity alterations during the interictal phase of migraine, however, there is discrepancy in the directionality of reports (i.e. increased vs. decreased connectivity) [17; 41; 46]. In our investigation, sumatriptan/naproxen infusion resulted in a reduction in DMN connectivity in

IS-induced intracranial nociception compared to controls. We previously investigated functional connectivity in response to repeated exposure of triptans, which is known to result in overuse headache, and found that prolonged administration resulted in increased DMN connectivity [4]. Duration of sumatriptan exposure may dictate efficacy and directionality of functional connectivity, and the combination of sumatriptan and naproxen may exhibit differential patterns of functional connectivity than sumatriptan alone.

The *basal ganglia network* is involved in pain processing through direct connectivity with sensory regions and integration of cortico-thalamic information [7], serving distinct roles in sensory, affective, cognitive, and modulatory pain processing domains [26]. Previous literature suggests that migraineurs exhibit increased basal ganglia functional connectivity [29; 47] compared to healthy controls and the degree of connectivity may be dependent on migraine frequency [26]. Similarly, we previously demonstrated a predominate increase in basal ganglia functional connectivity following IS migraine induction compared to sham treated animals [3]. Following sumatriptan/naproxen infusion we observed a global increase in basal ganglia network functional connectivity in IS treated animals compared to SIF controls suggesting that sumatriptan anti-migraine effects may not be due to mediation of basal ganglia connectivity. Although the basal ganglia possess 5-HT1b and 1d receptor subtypes [22], it is not known whether sumatriptan enacts its effects on this area.

Autonomic dysfunction is frequently reported in migraine studies [28], which is centrally mediated by a network of brain structures that are important for regulating the balance of sympathetic and parasympathetic systems [36]. We have previously demonstrated in rats that dural IS exposure increased resting state functional connectivity in key autonomic structures including the hippocampus, hypothalamus, and amygdala [3], and similar alterations in amygdala functional connectivity have been identified in clinical migraine populations [12]. Following sumatriptan/naproxen infusion, elevated hypothalamic and hippocampal connectivity remained compared to sham animals, however, a reduction in amygdala connectivity was identified. The amygdala facilitates both pro- and anti-nociceptive pathways by regulating affective components of pain as well as through direct anatomical connections to the periaqueductal grey (PAG) – an integral structure for descending pain modulation. Alternatively, sumatriptan may prevent activation of post-ganglionic parasympathetic neurons in the sphenopalatine ganglion through the interception their activation by trigeminal ganglia neurons [18].

The sensorimotor network includes primary- as well as association- motor and sensory structures that receive ascending trigeminovascular input via a trigemino-thalamo-cortical nociceptive pathway collectively encoding for spatial discrimination, intensity, and quality of migraine pain [8]. Triptan administration following migraine induction resulted in both increased and decreased sensorimotor network functional connectivity. Alterations in sensorimotor network connectivity has been demonstrated in clinical migraineurs, illustrated by weaker primary somatosensory (S1) connectivity [48]. This suggests that network dysfunction either underlies or develops in response to recurrent migraine attacks and successful pharmacological intervention may influence pain circuitry.

The salience network is involved in pain and analgesia for evaluating internal and external stimuli by integrating cognitive, emotional, and sensory information [6]. We have previously discovered global increases in salience network connectivity following migraine induction [3]. Pharmacological treatment with sumatriptan/naproxen infusion resulted in a predominate reduction in salience network connectivity within the hypothalamus, hippocampus, motor and sensory regions, and the olfactory amygdala compared to sham controls. Hallmarks of migraine often include increased sensitivity to light and odors. Consistent with these symptoms, BOLD fMRI measures are elevated within the amygdala in response to olfactory stimulation during untreated migraine [38]. Others have shown intra-network desynchronization within the amygdala of chronic migraineurs with and without medication overuse headache [1]. Changes in connectivity within the salience network, reported here, may underlie effective acute treatment strategies. Future work using chronic migraine models will be required to validate this interpretation provided that migraine may induce long-lasting network changes via recurrent over-sensitization and/or excitotoxicity.

Motor symptoms of migraine are well-characterized and include changes in coordination, dizziness, and ataxia, consistent with altered cerebellar structure and function [43]. In our preliminary investigation, migraine induced animals exhibited increased cerebellar network connectivity within pain related structures including the insula, somatosensory cortex, amygdala, hypothalamus, and hippocampus [3]. Subsequent sumatriptan/naproxen treatment in migraine induced animals did not yield regions of increased cerebellar connectivity compared to controls suggesting that aberrant activity in this network may be mitigated by successful migraine therapy.

Caveats

As with any translational study, there are a number of caveats that include:

1. *Does the imaging study support the human condition*? While symptoms of migraine, including aspects of pain and nausea, are impossible to evaluate in animals, the brain related changes provide an objective measure of neural circuits affected by a well-defined pre-clinical model. Furthermore, the responsivity to triptan/naproxen treatment intervention is consistent with the efficacy of the drug in humans.
2. *Animal Gender/Sex*: The current study used male rats to investigate the treatment of migraine pathophysiology. Given the prevalence of migraine is higher in females, a future set of experiments is necessitated in an independent cohort of both female-only and/or mixed sample. Moreover, pharmacological agents including sumatriptan have been shown to have distinct sexual dimorphism through actions on 5-HT receptor subtypes [2]. These influences could differentially impact network connectivity responses between sexes further validating the need for a future independent cohort.
3. *Awake MR Imaging*: The imaging in this study was conducted in conscious, non-anesthetized animals. Careful consideration was taken to mitigate potential movement related artifacts through training/exposing the animals to the imaging

holders and apparatuses prior to the experimental session. Anesthesia during MRI acquisition would confound both migraine induction and treatment while also suppressing neural activity. Because residual effects of anesthesia administered during setup may influence neural activity, even after consciousness is regained, all animals were exposed to identical levels and duration of anesthetic.

Conclusions

Here we build off of previous work to investigate brain network changes following pharmacological treatment for migraine-like pathophysiology. Using non-invasive MRI, we investigated functional connectivity changes following sumatriptan/naproxen – an agent widely used in clinical populations to provide migraine relief. The results presented here expand upon our understanding of how a successful pharmacological agent mitigates migraine by influencing network connectivity. Similar approaches can be implemented with other known therapies to compare mechanisms of action or potentially be used to develop novel migraine pharmacotherapies.

Acknowledgements

This research was supported by: Migraine Research Foundation (DB), Louis Herlands Fund for Pain Research (DB, LB). GlaxoSmithKline (Investigator Initiated Grant) (RB), and NIH grants NS069847 (RB), NS079678 (RB), K24-NS064050 (DB). The authors have no conflicts of interest to declare. Dr. Borsook consults to Biogen.

References

[1]. Androulakis XM, Rorden C, Peterlin BL, Krebs K. Modulation of salience network intranetwork resting state functional connectivity in women with chronic migraine. Cephalalgia 2018;38(11):1731–1741. [PubMed: 29237282]

[2]. Araldi D, Ferrari LF, Green P, Levine JD. Marked sexual dimorphism in 5-HT1 receptors mediating pronociceptive effects of sumatriptan. Neuroscience 2017;344:394–405. [PubMed: 28040566]

[3]. Becerra L, Bishop J, Barmettler G, Kainz V, Burstein R, Borsook D. Brain network alterations in the inflammatory soup animal model of migraine. Brain Res 2017;1660:36–46. [PubMed: 28167076]

[4]. Becerra L, Bishop J, Barmettler G, Xie Y, Navratilova E, Porreca F, Borsook D. Triptans disrupt brain networks and promote stress-induced CSD-like responses in cortical and subcortical areas. J Neurophysiol 2016;115(1):208–217. [PubMed: 26490291]

[5]. Becerra L, Pendse G, Chang PC, Bishop J, Borsook D. Robust reproducible resting state networks in the awake rodent brain. PLoS One 2011;6(10):e25701. [PubMed: 22028788]

[6]. Borsook D, Edwards R, Elman I, Becerra L, Levine J. Pain and analgesia: the value of salience circuits. Prog Neurobiol 2013;104:93–105. [PubMed: 23499729]

[7]. Borsook D, Maleki N, Becerra L, McEwen B. Understanding migraine through the lens of maladaptive stress responses: a model disease of allostatic load. Neuron 2012;73(2):219–234. [PubMed: 22284178]

[8]. Burstein R, Noseda R, Borsook D. Migraine: multiple processes, complex pathophysiology. J Neurosci 2015;35(17):6619–6629. [PubMed: 25926442]

[9]. Burstein R, Yamamura H, Malick A, Strassman AM. Chemical stimulation of the intracranial dura induces enhanced responses to facial stimulation in brain stem trigeminal neurons. J Neurophysiol 1998;79(2):964–982. [PubMed: 9463456]

[10]. Burstein R, Yarnitsky D, Goor-Aryeh I, Ransil BJ, Bajwa ZH. An association between migraine and cutaneous allodynia. Ann Neurol 2000;47(5):614–624. [PubMed: 10805332]

[11]. Capone ML, Tacconelli S, Sciulli MG, Anzellotti P, Di Francesco L, Merciaro G, Di Gregorio P, Patrignani P. Human pharmacology of naproxen sodium. J Pharmacol Exp Ther 2007;322(2):453–460. [PubMed: 17473175]

[12]. Chen Z, Chen X, Liu M, Dong Z, Ma L, Yu S. Altered functional connectivity of amygdala underlying the neuromechanism of migraine pathogenesis. J Headache Pain 2017;18(1):7. [PubMed: 28116559]

[13]. Coppola G, Di Renzo A, Tinelli E, Di Lorenzo C, Scapeccia M, Parisi V, Serrao M, Evangelista M, Ambrosini A, Colonnese C, Schoenen J, Pierelli F. Resting state connectivity between default mode network and insula encodes acute migraine headache. Cephalalgia 2018;38(5):846–854. [PubMed: 28605972]

[14]. Edelmayer RM, Vanderah TW, Majuta L, Zhang ET, Fioravanti B, De Felice M, Chichorro JG, Ossipov MH, King T, Lai J, Kori SH, Nelsen AC, Cannon KE, Heinricher MM, Porreca F. Medullary pain facilitating neurons mediate allodynia in headache-related pain. Ann Neurol 2009;65(2):184–193. [PubMed: 19259966]

[15]. Edwards KR, Rosenthal BL, Farmer KU, Cady RK, Browning R. Evaluation of sumatriptan-naproxen in the treatment of acute migraine: a placebo-controlled, double-blind, cross-over study assessing cognitive function. Headache 2013;53(4):656–664. [PubMed: 23406052]

[16]. Filippini N, MacIntosh BJ, Hough MG, Goodwin GM, Frisoni GB, Smith SM, Matthews PM, Beckmann CF, Mackay CE. Distinct patterns of brain activity in young carriers of the APOE-epsilon4 allele. Proc Natl Acad Sci U S A 2009;106(17):7209–7214. [PubMed: 19357304]

[17]. Hodkinson DJ, Veggeberg R, Kucyi A, van Dijk KR, Wilcox SL, Scrivani SJ, Burstein R, Becerra L, Borsook D. Cortico-Cortical Connections of Primary Sensory Areas and Associated Symptoms in Migraine. eNeuro 2016;3(6).

[18]. Ivanusic JJ, Kwok MMK, Ahn AH, Jennings EA. 5-HT(1D) receptor immunoreactivity in the sphenopalatine ganglion: implications for the efficacy of triptans in the treatment of autonomic signs associated with cluster headache. Headache 2011;51(3):392–402. [PubMed: 21352213]

[19]. Jakubowski M, Levy D, Kainz V, Zhang XC, Kosaras B, Burstein R. Sensitization of central trigeminovascular neurons: blockade by intravenous naproxen infusion. Neuroscience 2007;148(2):573–583. [PubMed: 17651900]

[20]. Jia Z, Tang W, Zhao D, Hu G, Li R, Yu S. Volumetric abnormalities of the brain in a rat model of recurrent headache. Mol Pain 2018;14:1744806918756466.

[21]. Jia Z, Tang W, Zhao D, Yu S. Disrupted functional connectivity between the periaqueductal gray and other brain regions in a rat model of recurrent headache. Sci Rep 2017;7(1):3960. [PubMed: 28638117]

[22]. Khoury CK, Couch JR. Sumatriptan-naproxen fixed combination for acute treatment of migraine: a critical appraisal. Drug Des Devel Ther 2010;4:9–17.

[23]. Kros L, Angueyra Aristizabal CA, Khodakhah K. Cerebellar involvement in migraine. Cephalalgia 2018;38(11):1782–1791. [PubMed: 29357683]

[24]. Levy D, Jakubowski M, Burstein R. Disruption of communication between peripheral and central trigeminovascular neurons mediates the antimigraine action of 5HT 1B/1D receptor agonists. Proc Natl Acad Sci U S A 2004;101(12):4274–4279. [PubMed: 15016917]

[25]. Levy D, Zhang XC, Jakubowski M, Burstein R. Sensitization of meningeal nociceptors: inhibition by naproxen. Eur J Neurosci 2008;27(4):917–922. [PubMed: 18333963]

[26]. Maleki N, Becerra L, Nutile L, Pendse G, Brawn J, Bigal M, Burstein R, Borsook D. Migraine attacks the Basal Ganglia. Mol Pain 2011;7:71. [PubMed: 21936901]

[27]. Maleki N, Linnman C, Brawn J, Burstein R, Becerra L, Borsook D. Her versus his migraine: multiple sex differences in brain function and structure. Brain 2012;135(Pt 8):2546–2559. [PubMed: 22843414]

[28]. Miglis MG. Migraine and Autonomic Dysfunction: Which Is the Horse and Which Is the Jockey? Curr Pain Headache Rep 2018;22(3):19. [PubMed: 29476276]

[29]. Moulton EA, Becerra L, Maleki N, Pendse G, Tully S, Hargreaves R, Burstein R, Borsook D. Painful heat reveals hyperexcitability of the temporal pole in interictal and ictal migraine States. Cereb Cortex 2011;21(2):435–448. [PubMed: 20562317]

[30]. Oshinsky ML, Gomonchareonsiri S. Episodic dural stimulation in awake rats: a model for recurrent headache. Headache 2007;47(7):1026–1036. [PubMed: 17635594]

[31]. Pardutz A, Schoenen J. NSAIDs in the Acute Treatment of Migraine: A Review of Clinical and Experimental Data. Pharmaceuticals (Basel) 2010;3(6):1966–1987. [PubMed: 27713337]

[32]. Pendse G, Borsook D, Becerra L. Enhanced false discovery rate using Gaussian mixture models for thresholding fMRI statistical maps. Neuroimage 2009;47(1):231–261. [PubMed: 19269334]

[33]. Peroutka SJ, McCarthy BG. Sumatriptan (GR 43175) interacts selectively with 5-HT1B and 5-HT1D binding sites. Eur J Pharmacol 1989;163(1):133–136. [PubMed: 2545459]

[34]. Pollock JM, Deibler AR, Burdette JH, Kraft RA, Tan H, Evans AB, Maldjian JA. Migraine associated cerebral hyperperfusion with arterial spin-labeled MR imaging. AJNR Am J Neuroradiol 2008;29(8):1494–1497. [PubMed: 18499796]

[35]. Raichle ME. The brain's default mode network. Annu Rev Neurosci 2015;38:433–447. [PubMed: 25938726]

[36]. Shields RW Jr. Functional anatomy of the autonomic nervous system. J Clin Neurophysiol 1993;10(1):2–13. [PubMed: 8458993]

[37]. Sinatra R Role of COX-2 inhibitors in the evolution of acute pain management. J Pain Symptom Manage 2002;24(1 Suppl):S18–27. [PubMed: 12204484]

[38]. Stankewitz A, May A. Increased limbic and brainstem activity during migraine attacks following olfactory stimulation. Neurology 2011;77(5):476–482. [PubMed: 21775739]

[39]. Steen KH, Steen AE, Reeh PW. A dominant role of acid pH in inflammatory excitation and sensitization of nociceptors in rat skin, in vitro. J Neurosci 1995;15(5 Pt 2):3982–3989. [PubMed: 7751959]

[40]. Strassman AM, Raymond SA, Burstein R. Sensitization of meningeal sensory neurons and the origin of headaches. Nature 1996;384(6609):560–564. [PubMed: 8955268]

[41]. Tessitore A, Russo A, Giordano A, Conte F, Corbo D, De Stefano M, Cirillo S, Cirillo M, Esposito F, Tedeschi G. Disrupted default mode network connectivity in migraine without aura. J Headache Pain 2013;14:89. [PubMed: 24207164]

[42]. Tso AR, Trujillo A, Guo CC, Goadsby PJ, Seeley WW. The anterior insula shows heightened interictal intrinsic connectivity in migraine without aura. Neurology 2015;84(10):1043–1050. [PubMed: 25663219]

[43]. Vincent M, Hadjikhani N. The cerebellum and migraine. Headache 2007;47(6):820–833. [PubMed: 17578530]

[44]. Wieseler J, Ellis A, Sprunger D, Brown K, McFadden A, Mahoney J, Rezvani N, Maier SF, Watkins LR. A novel method for modeling facial allodynia associated with migraine in awake and freely moving rats. J Neurosci Methods 2010;185(2):236–245. [PubMed: 19837113]

[45]. Xue T, Yuan K, Cheng P, Zhao L, Zhao L, Yu D, Dong T, von Deneen KM, Gong Q, Qin W, Tian J. Alterations of regional spontaneous neuronal activity and corresponding brain circuit changes during resting state in migraine without aura. NMR Biomed 2013;26(9):1051–1058. [PubMed: 23348909]

[46]. Xue T, Yuan K, Zhao L, Yu D, Zhao L, Dong T, Cheng P, von Deneen KM, Qin W, Tian J. Intrinsic brain network abnormalities in migraines without aura revealed in resting-state fMRI. PLoS One 2012;7(12):e52927. [PubMed: 23285228]

[47]. Yuan K, Zhao L, Cheng P, Yu D, Zhao L, Dong T, Xing L, Bi Y, Yang X, von Deneen KM, Liang F, Gong Q, Qin W, Tian J. Altered structure and resting-state functional connectivity of the basal ganglia in migraine patients without aura. J Pain 2013;14(8):836–844. [PubMed: 23669074]

[48]. Zhang J, Su J, Wang M, Zhao Y, Zhang QT, Yao Q, Lu H, Zhang H, Li GF, Wu YL, Liu YS, Liu FD, Zhuang MT, Shi YH, Hou TY, Zhao R, Qiao Y, Li J, Liu JR, Du X. The sensorimotor network dysfunction in migraineurs without aura: a resting-state fMRI study. J Neurol 2017;264(4):654–663. [PubMed: 28154971]

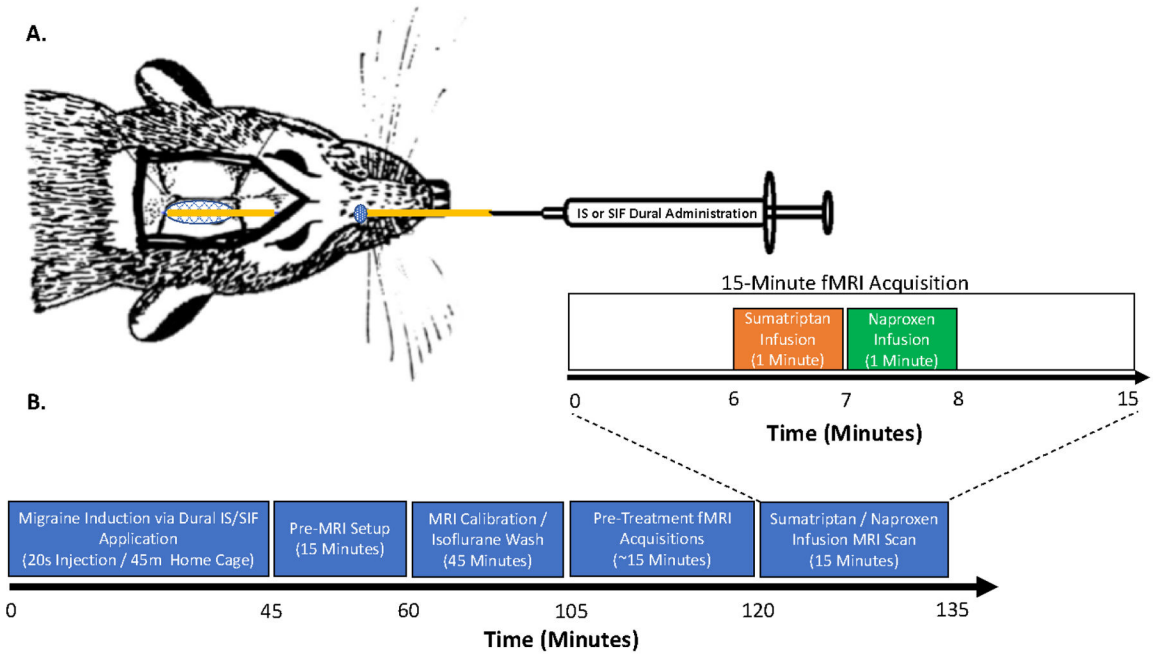

Figure 1. Experimental Design and Setup.

Infusion and Timing of Treatments. (A) A catheter was surgically implanted through a cranial window made adjacent to the lambda suture. The loose end of the catheter was routed subcutaneously exiting the skin in the medial facial region to allow for either IS or SIF dural application. (B) Experimental timeline: IS or SIF was applied to the dura mater of each animal and then returned to their home-cage for forty five minutes. Next, a fifteen-minute MRI setup was then performed while the animal was under 2% isoflurane. During this time, the animals were placed in the imaging holder and a tail-vein catheter was inserted. After setup, the animal was placed in the MRI to calibrate the magnet and acquire structural (T1) scans. Functional MRI scanning started forty-five minutes after the completion of the pre-MRI setup to mitigate any residual effects of isoflurane. Migraine treatment was captured during a fifteen-minute fMRI scan with infusion of sumatriptan (1mg/kg) and then naproxen (1mg/kg) independently over the course of one minute, to prevent potential precipitation of the drug if mixed.

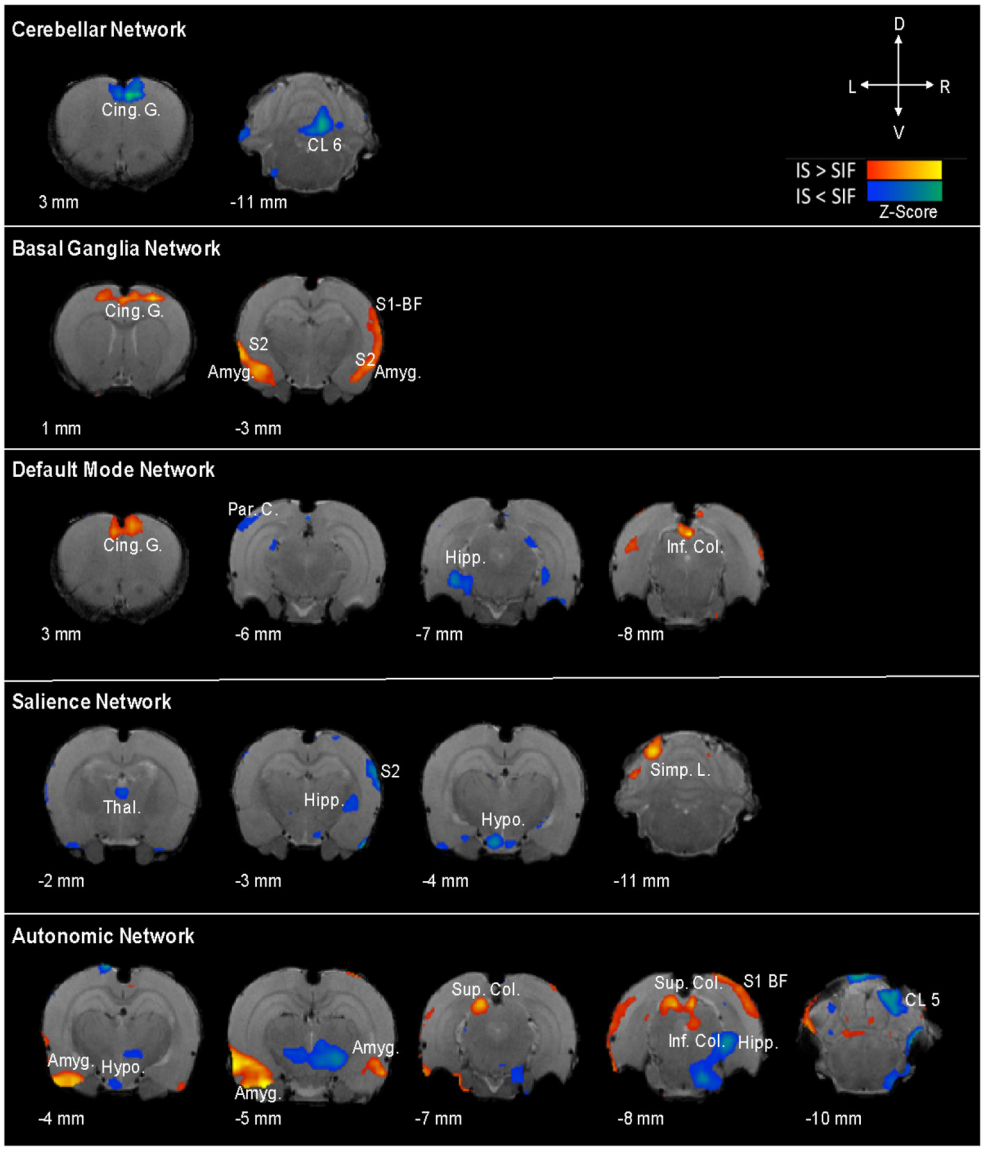

Figure 2. Network Alterations Following Sumatriptan-Naproxen Infusion in IS vs. SIF Animals.

Whole-brain network alterations following sumatriptan-naproxen infusion in IS vs. SIF animals. Sumatriptan-naproxen infusion resulted in differential activation across brain networks in the migraine-like condition (IS) compared to the SIF (control) animals. Significant changes in connectivity were identified across a number of different networks including the cerebellar, basal ganglia, default mode, salience, and autonomic networks. Specifically, changes in connectivity between IS and SIF groups were revealed in a number of cortical and subcortical regions involved in migraine pathophysiology including the amygdala, hypothalamus, hippocampus, thalamus, cingulate, and somatosensory cortices. For a complete list of network changes refer to Table(s) 1–6.

Table 1:

Cerebellar Network (CN)

Region	Zstat	X(mm)	Y(mm)	Z(mm)	Volume	Laterality
IS > SIF						
No significant differences						
IS<SIF						
Cingulate Cortex	2.48	−0.23	7.62	2.00	2.61	L
Cerebellum Lobule_03	2.45	0.59	4.92	−11.00	8.08	R
Spinal Trigeminal Nuclei	2.27	1.76	2.46	−14.00	31.11	R
Corpus Callosum	2.94	−0.70	7.62	−6.00	3.19	L
Somatosensory Cortex Primary Forelimb Region	2.19	2.93	8.09	0.00	2.18	R
Visual Cortex Secondary	2.10	4.22	7.73	−7.00	9.57	R
Cerebellum Lobule 02	1.98	−0.23	4.45	−11.00	2.11	L
Motor Cortex Secondary	1.85	1.41	8.44	2.00	4.44	R
Olfactory Cortex Lateral	1.71	−5.86	1.29	−2.00	1.14	L
Cerebellum Lobule 06	1.47	0.94	6.91	−12.00	1.48	R
Olfactory Cortex Lateral	2.00	5.27	1.64	−4.00	4.13	R

Table 2:

Default Mode Network (DMN)

Region	Zstat	X(mm)	Y(mm)	Z(mm)	Volume	Laterality
IS>SIF						
Cingulate Cortex	3.46	−0.23	7.62	2.00	5.19	L
Spinal Trigeminal Nuclei	2.87	1.76	2.11	−14.00	1.70	R
Motor Cortex Secondary	2.74	0.59	8.09	2.00	7.21	R
Amygdaloid Nuclear Complex Laterobasal	2.51	3.75	1.64	−5.00	2.20	R
Inferior Colliculus	4.10	−1.05	7.27	−9.00	7.77	L
IS<SIF						
Cerebellum Lobule 06	1.96	−1.05	8.09	−12.00	3.27	L
Hippocampal Formation Subicular Complex	1.94	−4.57	2.93	−7.00	1.84	L
Simple Lobule	1.88	−4.69	5.74	−10.00	1.69	L
Somatosensory Cortex Primary Trunk Region	1.84	2.58	8.09	−3.00	1.14	R
Somatosensory Cortex Primary Trunk Region	1.79	1.76	7.73	−3.00	1.40	R
Ansiform Lobule Crus 2	1.78	−5.51	5.62	−12.00	1.41	L
Nucleus of the Lateral Lemniscus	1.83	−3.05	2.93	−9.00	2.49	L
Somatosensory Cortex Primary Jaw Region	1.94	4.10	6.91	1.00	2.98	R
Auditory Cortex Primary	1.68	−6.21	4.10	−4.00	1.24	L
Perirhinal Cortex	1.47	5.74	2.93	−8.00	2.61	R
Parietal Cortex Posterior Area	1.43	−5.86	7.73	−6.00	1.28	L

Table 3:

Basal Ganglia Network (BGN)

Region	Zstat	X(mm)	Y(mm)	Z(mm)	Volume	Laterality
IS>SIF						
Simple Lobule	2.82	3.75	6.56	−10.00	3.76	R
Motor Cortex Primary	2.81	2.58	7.73	1.00	1.43	R
Cerebellum Lobule 05	2.65	2.11	7.62	−10.00	2.25	R
Perirhinal Cortex	2.56	−6.68	2.81	−3.00	3.06	L
Olfactory Cortex Lateral	2.54	5.74	1.76	−4.00	4.06	R
Auditory Cortex Secondary	2.79	6.09	3.28	−4.00	6.28	R
Amygdaloid Nuclear Complex Laterobasal	2.39	−5.04	1.64	−3.00	7.86	L
Temporal Association Cortex	2.86	−5.86	6.09	−9.00	18.44	L
Ventral Pallidum	1.98	1.76	0.94	0.00	1.96	R
Visual Cortex Primary	1.97	−2.23	8.44	−9.00	1.48	L
Cingulate Cortex	2.10	0.12	7.62	1.00	2.46	R
Amygdaloid Nuclear Complex Laterobasal	1.75	4.57	0.94	−3.00	1.18	R
Somatosensory Cortex Secondary	1.71	6.21	5.27	−3.00	6.39	R
Somatosensory Cortex Primary	1.65	4.92	7.73	−5.00	2.93	R
Somatosensory Cortex Primary Barrel Field	1.52	5.74	6.44	−3.00	4.06	R
Olfactory Cortex Lateral	1.50	3.40	3.28	−9.00	4.48	R
Motor Cortex Primary	1.96	−3.05	7.73	2.00	5.25	L
Somatosensory Cortex Primary Forelimb Region	1.46	2.58	8.44	−2.00	1.72	R
Olfactory Amygdala	1.44	−5.04	1.64	−5.00	1.41	L
Paramedian Lobule	1.47	1.41	6.91	−14.00	9.72	R
Paramedian Lobule	1.33	−2.23	7.73	−14.00	2.43	L
IS<SIF						
No significant differences						

Table 4:

Autonomic Network (AN)

Region	Zstat	X(mm)	Y(mm)	Z(mm)	Volume	Laterality
IS>SIF						
Vomeronasal Amygdala	4.88	−4.22	1.64	−6.00	10.22	L
Paramedian Lobule	2.91	−3.05	6.80	−14.00	1.51	L
Paramedian Lobule	2.77	2.93	6.80	−14.00	4.56	R
Paraflocculus	2.69	−5.04	4.45	−11.00	12.85	L
Superior Colliculus	2.56	−1.87	6.91	−7.00	1.66	L
Hippocampal Formation CA1 Field	2.51	4.57	1.99	−6.00	1.66	R
Vomeronasal Amygdala	2.45	3.40	1.29	−6.00	1.26	R
Somatosensory Cortex Primary Barrel Field	2.35	−4.22	7.73	−2.00	1.10	L
Olfactory Cortex Lateral	2.26	5.74	1.64	−5.00	1.41	R
Ansiform Lobule Crus 2	2.23	3.75	4.92	−12.00	6.07	R
Cerebellum Lobule 07	2.01	0.12	8.09	−14.00	2.21	R
Cranial Special Sensory Nuclei	1.91	−4.22	2.46	−11.00	2.88	L
IS<SIF						
Inferior Colliculus	3.17	1.41	7.27	−9.00	7.03	R
Cerebellum Lobule 05	2.67	2.11	7.62	−10.00	1.65	R
Retrosplenial Cortex	2.39	2.93	6.91	−9.00	3.91	R
Olfactory Cortex Lateral	2.32	−3.87	4.45	−9.00	1.95	L
Simple Lobule	1.93	−3.75	6.44	−10.00	1.29	L
Olfactory Cortex Lateral	1.92	4.92	1.99	−3.00	1.13	R
Hypothalamus Periventicular Zone	1.80	−0.94	0.12	−4.00	3.56	L
Olfactory Cortex Lateral	1.67	−4.69	2.11	0.00	2.76	L
Reticular Formation Midbrian_	1.64	−3.40	4.92	−7.00	1.06	L
Perirhinal Cortex	1.89	6.09	2.81	−3.00	3.13	R
Cerebellum Lobule 05	1.51	−2.34	8.09	−10.00	8.84	L
Hippocampal Formation Subicular Complex	2.56	3.28	3.98	−8.00	81.30	R
Olfactory Cortex Lateral	1.63	4.10	1.76	1.00	3.90	R
Visual Cortex Secondary	1.42	−2.23	8.55	−5.00	3.09	L
Somatosensory Cortex Primary Forelimb Region	1.60	3.40	6.91	0.00	2.75	R
Parietal Cortex Posterior Area	1.35	−3.40	8.55	−5.00	1.50	L

Table 5:

Sensorimotor Network (SMN)

Region	Zstat	X(mm)	Y(mm)	Z(mm)	Volume	Laterality
IS>SIF						
Cerebellum Lobule_07	2.62	−2.58	7.27	−13.00	10.35	L
Spinal Trigeminal Nuclei	2.08	2.11	2.46	−14.00	1.24	R
Ansiform Lobule Crus 2	2.04	−4.22	6.44	−13.00	1.47	L
Somatosensory Cortex Primary Hindlimb Region	2.03	1.41	7.62	−1.00	7.54	R
Thalamus Posterior Nucleus	1.95	1.76	4.10	−3.00	1.84	R
Ansiform Lobule Crus 2	1.94	−5.04	6.44	−13.00	0.45	L
Raphe Nuclei Midbrain	1.88	−0.23	4.10	−9.00	2.36	L
Ansiform Lobule Crus 2	1.83	−5.39	5.27	−13.00	1.58	L
Cerebellum Lobule 09	1.77	−3.05	4.10	−14.00	2.93	L
Paramedian Lobule	1.74	−4.69	5.27	−13.00	0.58	L
Temporal Association Cortex	1.74	−5.86	4.92	−8.00	1.84	L
Olfactory Cortex Lateral	1.66	−5.51	0.12	−3.00	2.76	L
Motor Cortex Primary	1.66	1.76	8.09	1.00	1.46	R
Cingulate Cortex	1.63	0.59	7.27	1.00	2.21	R
Copula of the Pyramis	1.63	−3.52	4.10	−13.00	2.88	L
Visual Cortex Primary	1.61	−4.22	7.62	−8.00	0.73	L
Somatosensory Cortex Primary Upper Lip Region	1.57	4.92	4.45	1.00	4.08	R
Visual Cortex Secondary	1.81	−5.04	7.62	−7.00	1.51	L
Somatosensory Cortex Primary Trunk Region	1.49	−3.40	8.09	−4.00	0.38	L
Inferior Colliculus	1.48	0.59	6.09	−9.00	0.48	R
Somatosensory Cortex Secondary	1.78	−6.33	6.44	−4.00	1.24	L
Hypothalamus Lateral Zone	1.43	0.59	0.82	−4.00	1.50	R
Somatosensory Cortex Primary Upper Lip Region	1.71	−5.86	6.09	0.00	11.51	L
Cerebellum Lobule 07	2.24	0.59	7.73	−14.00	19.57	R
Superior Colliculus	1.41	2.11	6.09	−7.00	1.00	R
Somatosensory Cortex Secondary	1.73	4.92	4.57	−1.00	3.75	R
Olfactory Cortex Lateral	1.68	5.39	1.29	−6.00	1.74	R
Cerebellum Lobule 02	2.52	2.58	4.10	−10.00	5.42	R
Somatosensory Cortex Primary Hindlimb Region	1.87	−2.34	8.09	−1.00	1.70	L
IS<SIF						
Motor Cortex Secondary	3.41	0.94	8.91	−4.00	1.61	R
Perirhinal Cortex	2.87	−6.21	3.28	−4.00	2.27	L
Perirhinal Cortex	2.74	−5.86	2.46	−4.00	2.54	L
Visual Cortex Secondary	2.71	1.76	8.55	−7.00	4.26	R
Motor Cortex Primary	2.44	−1.41	9.37	−3.00	3.09	L
Superior Colliculus	2.16	−0.59	6.09	−6.00	1.70	L
Inferior Colliculus	2.70	−1.41	6.91	−9.00	8.82	L
Septal Region Lateral Group	1.96	−0.70	5.74	−1.00	1.07	L

Region	Zstat	X(mm)	Y(mm)	Z(mm)	Volume	Laterality
Pretectum	1.89	1.41	4.80	−5.00	0.45	R
Trigeminal Nerve	1.69	2.11	0.82	−8.00	0.81	R
Perirhinal Cortex	2.03	6.21	2.93	−3.00	1.62	R

Table 6:

Salience Network (SN)

Region	Zstat	X(mm)	Y(mm)	Z(mm)	Volume	Laterality
IS>SIF						
Simple Lobule	3.68	−3.52	7.62	−11.00	1.77	L
Simple Lobule	3.19	−5.04	5.62	−10.00	1.41	L
IS<SIF						
Cerebellum Lobule 07	2.30	−1.87	7.73	−14.00	4.71	L
Hypothalamus Medial Zone	2.11	−1.05	0.47	−4.00	5.20	L
Olfactory Amygdala	1.99	−5.04	1.64	−5.00	7.44	L
Somatosensory Cortex Secondary	1.85	6.21	5.74	−3.00	1.90	R
Olfactory Cortex Lateral	1.66	−3.87	2.11	1.00	4.67	L
Paraflocculus	1.62	−5.51	3.98	−12.00	1.83	L
Temporal Association Cortex	2.19	−6.21	5.62	−8.00	11.12	L
Superior Colliculus	2.12	−1.05	7.27	−8.00	4.05	L
Thalamus Intralaminar Nuclei	1.37	−0.23	4.10	−2.00	1.02	L
Somatosensory Cortex Secondary	1.36	5.39	3.63	0.00	1.00	R
Motor Cortex Secondary	1.34	−1.05	8.09	1.00	4.61	L
Hippocampal Formation CA1 Field	2.14	4.57	1.99	−6.00	7.42	R
Olfactory Cortex Lateral	2.61	−3.87	3.28	−8.00	15.72	L
Motor Cortex Secondary	1.31	−1.41	8.44	1.00	3.17	L
Somatosensory Cortex Primary Jaw Region Oral Surface	1.24	−5.39	6.44	1.00	1.69	L
Ansiform Lobule Crus 2	1.51	3.05	4.92	−12.00	38.69	R